Ore Geology Reviews 71 (2015) 305–317

Contents lists available at ScienceDirect

Ore Geology Reviews

journal homepage: www.elsevier.com/locate/oregeorev

Precise zircon U–Pb and molybdenite Re–Os dating of the Shuikoushan granodiorite-related Pb–Zn mineralization, southern Hunan, South China

Jin-Chuan Huang [a,b], Jian-Tang Peng [a,c,*], Jie-Hua Yang [a], Bang-Lu Zhang [a,b], Chun-Xia Xu [a,b]

[a] State Key Laboratory of Ore Deposit Geochemistry, Institute of Geochemistry, Chinese Academy of Sciences, Guiyang 550002, PR China
[b] University of Chinese Academy of Sciences, Beijing 10049, PR China
[c] Key Laboratory of Metallogenic Prediction of Nonferrous Metals, Ministry of Education, School of Geosciences and Info-physics, Central South University, Changsha 410083, PR China

ARTICLE INFO

Article history:
Received 2 January 2015
Received in revised form 13 June 2015
Accepted 14 June 2015
Available online 16 June 2015

Keywords:
SIMS U–Pb dating
Re–Os dating
Molybdenite
Pb–Zn mineralization
Southern Hunan
South China

ABSTRACT

The Shuikoushan ore district, located in southern Hunan Province, South China, contains Pb–Zn–Au mineralization hosted in the Devonian to Triassic strata and Mesozoic granodiorite intrusions. Ore minerals are mainly pyrite, sphalerite, galena and minor molybdenite. Molybdenite, usually intergrown with pyrite, formed during Pb–Zn hydrothermal mineralization. In order to determine the precise age of Pb–Zn mineralization and further understand the relationship between magma emplacement and hydrothermal mineralization in the ore district, molybdenite Re–Os dating and zircon SIMS U–Pb dating were undertaken. The zircon U–Pb dating reveals that the granodiorite intrusion was emplaced at 158.8 ± 1.8 Ma (MSWD = 0.40). Re–Os isotopic age of seven molybdenite samples yields model ages ranging from 157.5 ± 2.5 Ma to 161.0 ± 2.4 Ma, and gives a well-defined ^{187}Re–^{187}Os isochron age of 157.8 ± 1.4 Ma (2σ, MSWD = 1.3), indicating the timing of Pb–Zn mineralization in the Shuikoushan ore district at about 158 Ma. This date coincides well with the zircon SIMS U–Pb age of the granodiorite, revealing a genetic association between the Pb–Zn mineralization and the granitic magmatism. Combined with geochronological data published for other Pb–Zn–(Cu) deposits in southern Hunan, it can be concluded that the granodiorite-related Pb–Zn mineralization throughout southern Hunan mainly occurred at 160–156 Ma, rather than 180–170 Ma or 170–160 Ma as considered previously. The Pb–Zn mineralization and major W–Sn mineralization in southern Hunan are coeval and may be related to the same geological event.

1. Introduction

Mesozoic granitoids are widespread in the Nanling Range, South China, and are temporally and spatially closely related to Pb, Zn, W and Sn mineralization. Generally speaking, Pb–Zn deposits are usually related to small granodiorite intrusions, whereas those W–Sn deposits are associated with granite plutons (Hua et al., 2003; Mao et al., 2008; Xu et al., 1982, 1983). Historically, the W–Sn mineralization and the Pb–Zn mineralization related to granitic intrusions in the area were considered to have formed during two different metallogenic systems (Hua et al., 2003; Mao et al., 2008; Xu et al., 1982, 1983).

Extensive research has been performed on W–Sn deposits and related granite plutons in the Nanling Range (e.g. Hsu, 1943; Liu, 1980; Lu, 1986; Mao et al., 1998; Mo et al., 1958; RGNTD, 1985; Wang et al., 1987; Xu and Ding, 1938; Zhu et al., 1981). Recent studies have constrained the timing of W–Sn mineralization in the region through precise geochronological analyses (e.g. Cai et al., 2006; Feng et al., 2011; Fu et al., 2007; Guo et al., 2011; Hu et al., 2012; Liu et al., 2008a, 2012; Mao et al., 2007; Peng et al., 2006, 2007; Qi et al., 2012; Wang et al., 2004; Yuan et al., 2008, 2011). Three main episodes of Mesozoic granite-related W–Sn mineralization have been defined (Mao et al., 2007, 2013), including Late Triassic (230–210 Ma), Mid–Late Jurassic (160–150 Ma) and Early–Mid-Cretaceous (120–80 Ma). The 160–150 Ma event was the most important W–Sn mineralization throughout the Nanling Range (Mao et al., 2007, 2013; Peng et al., 2006, 2008), and has been determined to be coeval with granitoid magmatism (Peng et al., 2008). In contrast, the Pb–Zn mineralization and related granodiorite intrusions in the Nanling Range have received less attention; precise ages for Pb–Zn mineralization are relatively scarce (Lu et al., 2006; Yuan, 2013). Existing inferred ages are considered to be 180–170 Ma (Hua et al., 2005) or 170–160 Ma (Mao et al., 2008, 2013).

The Shuikoushan ore district hosts Pb–Zn mineralization related to the granodiorite intrusions of the Nanling Range. The district contains total metal reserves of 874,600 t Pb and 1,110,800 t Zn, with an average grade of 2.50–3.92% Pb and 2.57–4.40% Zn, respectively (Zhu, 1999). As an important Pb- and Zn-producer in China for the past century, the geological characteristics, ore genesis and geochemical characteristics of the Shuikoushan ore district and related intrusions have attracted much attention (e.g. Li and Peng, 1996; Liu, 1994; Liu and Tan, 1996; Lu et al., 2013; Ma et al., 2006; Tan and Wan, 2008; Yu and Liu, 1997; Zeng et al., 2000; Zhang, 1957). However, due to lack of reliable ages,

* Corresponding author at: State Key Laboratory of Ore Deposit Geochemistry, Institute of Geochemistry, Chinese Academy of Sciences, Guiyang 550002, PR China.
E-mail address: jtpeng@126.com (J.-T. Peng).

http://dx.doi.org/10.1016/j.oregeorev.2015.06.011
0169-1368/

it is still unclear when Pb–Zn mineralization took place, and the emplacement timing of the ore-related intrusion is still controversial (172–143 Ma, Ma et al., 2006; Wang et al., 2002; Yu and Liu, 1997; Zuo et al., 2014), precluding the confident assessment of the genetic association between Pb–Zn mineralization and pluton emplacement. For the first time, we report precise ages for Pb–Zn mineralization in the Shuikoushan district based on molybdenite Re–Os data, as well as the timing of emplacement for granodiorite intrusions in the district using zircon SIMS U–Pb analysis.

2. Geological background

South China consists of the Yangtze Block to the northwest and the Cathaysian Block to the southeast, separated by the Qin-Hang Neoproterozoic suture, and bounded by the North China Block to the north (Fig. 1). The basement of the Yangtze Block is composed of Archean to Proterozoic rocks overlain by a sequence of Neoproterozoic (Sinian) to Mesozoic sedimentary cover (Chen and Jahn, 1998). The basement of Cathaysian Block consists of Precambrian rocks overlain by Sinian to Mesozoic cover sedimentary successions (Chen and Jahn, 1998).

Mesozoic granitoids are widespread in the Nanling Range (Fig. 1) (IGCAS, 1979; Mo et al., 1980; Zhou et al., 2006), and economically significant metallic mineralization in the region is genetically associated with these granitic rocks. These intrusions predominately consist of biotite granite with peraluminous compositions and relatively high initial $^{87}Sr/^{86}Sr$ ratios of 0.710–0.735, which were widely considered to be of S-type (IGCAS, 1979; Mo et al., 1980; Xu et al., 1983), but recently some have been re-identified as highly-fractionated I-type or A-type granites (e.g. Bai et al., 2005; Fu et al., 2005; Jiang et al., 2006, 2008; Li et al., 2007a). In addition, these intrusions include small granodiorite intrusions with metaluminous to weak peraluminous compositions and relatively low initial $^{87}Sr/^{86}Sr$ ratios of 0.707–0.711, which were regarded as I-type granites (Huang et al., 2015; Wang et al., 2003).

As an important part of the Nanling Range, southern Hunan hosts W–Sn and Pb–Zn ore bodies associated with Mesozoic granitoids (Fig. 1). The major W–Sn deposits related to granite plutons in the area include the Shizhuyuan W–Sn–Mo–Bi deposit (Mao and Li, 1995, 1996), Yaogangxian W deposit (Peng et al., 2006), Xianghualing Sn deposit (Yuan et al., 2008) and Furong Sn deposit (Li et al., 2007b; Peng et al., 2007; Yuan et al., 2011), representing the largest W–Sn metallogenic belt in the world (Mao et al., 2007). Three types of W–Sn mineralization, including greisen-, skarn-, and quartz vein-type, are widespread in the area. Geochronological data indicated that W–Sn mineralization in the area occurred during 160–150 Ma (Mao et al., 2007, 2013; Peng et al., 2006, 2008). In comparison, major Pb–Zn deposits, usually are associated with I-type granodiorite intrusions, examples include the Shuikoushan Pb–Zn–Au deposit (Li and Peng,

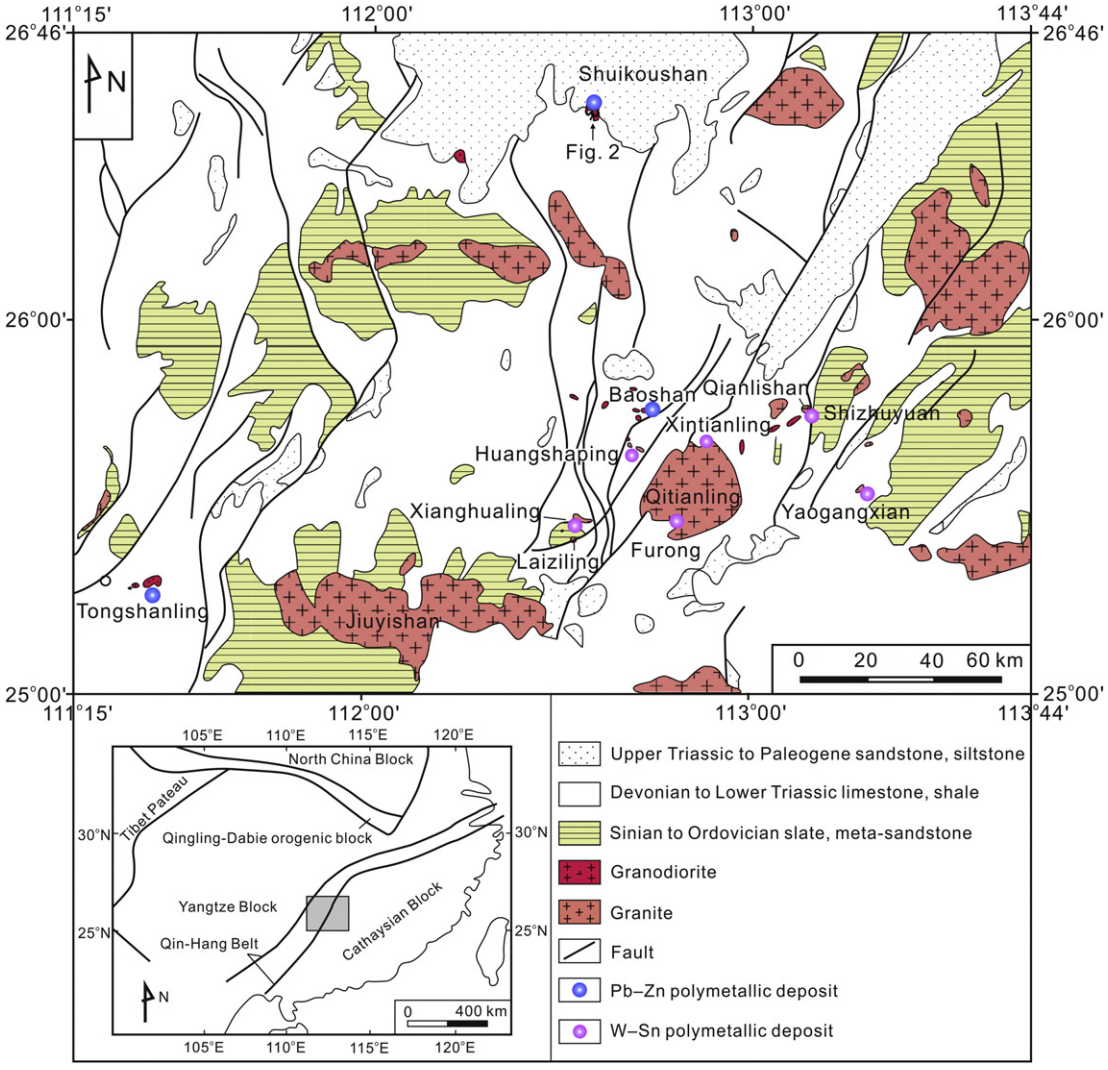

Fig. 1. Distribution of important Pb–Zn and W–Sn deposits in southern Hunan, South China. Modified after Wang et al. (2003) and Peng et al. (2006).

1996), Baoshan Pb–Zn–Cu deposit (Lu et al., 2006) and Tongshanling Cu–Pb–Zn deposit. The Pb–Zn mineralization in the area is mostly hydrothermal filling type (e.g. Shuikoushan) and skarn type (e.g. Tongshanling) (Wang et al., 1988).

3. Ore deposit geology

The Shuikoushan ore district is located about 40 km away from Hengyang city, Hunan Province. It is situated at the southern margin of Hengyang Cretaceous red-bed basin (Fig. 2). The stratigraphic sequence in the mining district consists of Devonian limestone, Carboniferous limestone–dolomite, Lower Permian limestone (Qixia Fm.), marlstone, argillaceous shale and siliceous rocks (Dangchong Fm.), Upper Permian shale, siltstone (Douling Fm.) and Lower Triassic limestone with marl and shale layers, unconformably overlain by Jurassic and Cretaceous sandstone–shale rocks. As a result of the Triassic and Jurassic tectonic events, sedimentary units of Devonian to Permian ages have been folded and locally overturned and brecciated (Figs. 2, 3).

Numerous intrusive rocks are exposed in the Shuikoushan mining district; they have a total exposed area of 4.8 km^2 (Fig. 2). Among them, the Shuikoushan granodiorite is the most important; it intruded Permian carbonate rocks during the Jurassic period (Fig. 3a) (Ma et al., 2006; Wang et al., 2002; Zuo et al., 2014). This intrusion is medium-grained biotite granodiorite, with SiO_2 ranging from 62.0 to 65.2 wt.%, Al_2O_3 from 15.0 to 17.5 wt.%, $K_2O + Na_2O$ from 5.60 to 7.55 wt.%, $K_2O/Na_2O > 1$, and A/CNK most <1.1 (Huang et al., 2015; Wang et al., 2003; Yu and Liu, 1997). They are metaluminous to weak peraluminous rocks, belonging to high-K calc-alkaline series and are usually considered to be of I-type (Huang et al., 2015; Wang et al., 2003; Yu and Liu, 1997).

Within the Shuikoushan ore district, the Shuikoushan Pb–Zn–Au deposit is one of the most important deposits in the area, which consists of the Laoyachao Pb–Zn–Au ore block and Yagongtang Pb–Zn–Au ore block (Fig. 3a). The Pb and Zn mineralization in the Shuikoushan Pb–Zn–Au deposit mainly occurs in the fractured zones between the limestone in the Qixia Fm. and the granodiorite intrusions, whereas Au mineralization occurs in the cryptoexplosive breccia belt between the granodiorite and marl and siliceous rocks of the Dangchong Fm. (Fig. 3b) (Li and Peng, 1996). The Pb–Zn mineralization in the Shuikoushan deposit is of hydrothermal fracture filling type. Skarn is generally absent and just locally occurs in the contact zone between the granodiorite intrusion and the carbonate rocks and contains no economically significant mineralization.

The Laoyachao Pb–Zn–Au mining district comprises 16 orebodies, with predominantly lens-shaped, cystic and tubular shapes. Individual orebodies in the mining district are up to 302 m long and 38 m wide and typically extend for about 80 to 420 m downdip. The Yagongtang mining district consists of 10 orebodies, with lens-shaped and stratiform-like shapes. Individual orebodies in the district are up to 1200 m long and 28 m wide and typically extend for about 50 to 520 m downdip.

Ore minerals in the Shuikoushan Pb–Zn–Au deposit include pyrite, sphalerite and galena, with minor molybdenite and chalcopyrite. Gangue minerals in the deposit are dominated by quartz, calcite and fluorite with minor dolomite and clay minerals. Mineral assemblages, ore textures as well as vein crosscutting relationships indicate that Pb–Zn mineralization in the area can be divided into three stages, early pyrite–quartz stage, sphalerite–galena–pyrite–quartz stage and late carbonate stage (Fig. 4).

The early pyrite–quartz stage consists mainly of disseminated or massive pyrite with minor chalcopyrite, molybdenite (Fig. 5a–d), sphalerite, galena (Fig. 5e), quartz (Fig. 5f), calcite and fluorite. Pyrite mostly appears as euhedral–anhedral grains with variable sizes and commonly occurs as densely disseminated or massive textures associated with minor quartz and calcite (Fig. 5e, f). Molybdenite occurs as veins or appears with disseminated pyrite and chalcopyrite in the altered granodiorite intrusion (Fig. 5a–d). Few sphalerite and galena grains are disseminated in the massive ores (Fig. 5e).

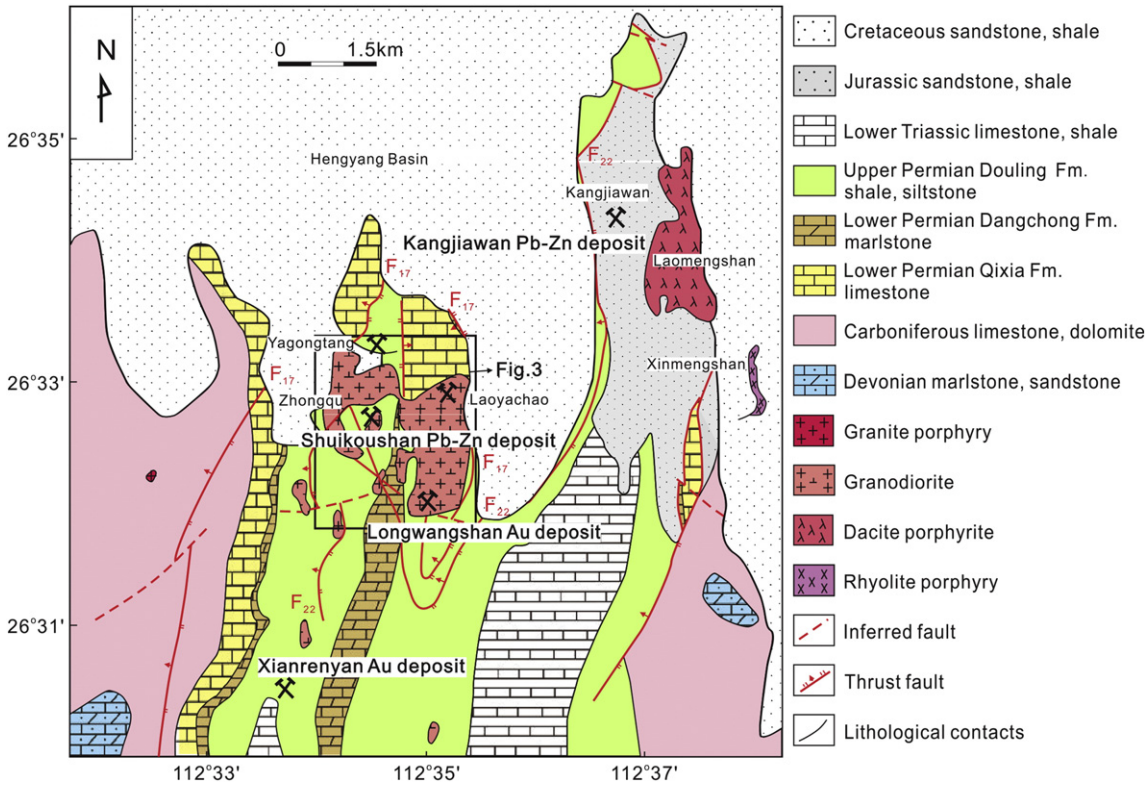

Fig. 2. Geological map for the Shuikoushan Pb–Zn–Au ore district, South China. Modified after Li and Peng (1996).

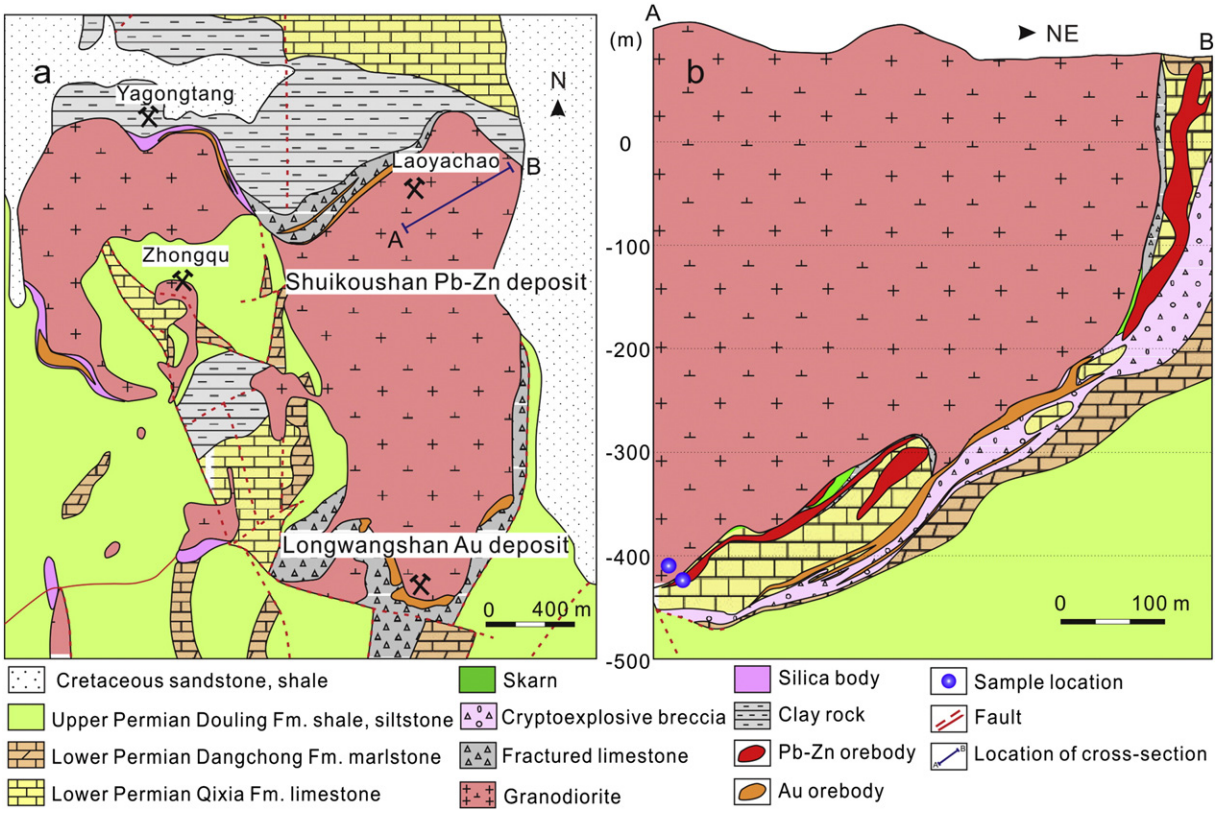

Fig. 3. Geological map (a) and cross-section map (b) for the Shuikoushan Pb–Zn–Au deposit, South China.

The sphalerite–galena–pyrite–quartz stage is characterized by the widespread occurrence of sphalerite, galena and pyrite with minor chalcopyrite, calcite, quartz and fluorite (Fig. 5g, h). Sphalerite is brown and irregularly shaped, and is usually intergrown with galena. Minor chalcopyrite occurs as exsolution texture in sphalerite. Sphalerite and galena often occur as the infilling of fractures in pyrite or as subhedral to euhedral crystals associated with pyrite (Fig. 5h).

The later carbonate stage mainly forms calcite and minor fluorite, which fills fissures in the early ores, or occurs in the vugs (Fig. 5e).

4. Sampling and analytical methods

4.1. Zircon U–Pb dating

Sample SKS-36 was collected from the granodiorite intrusion in the Laoyachao mining district, free of weathering and alteration. Zircons were separated by conventional heavy liquid and magnetic techniques at the mineral separation laboratory of Langfang Regional Geological Survey, Hebei Province. Zircon grains, together with zircon standard

Stage / Mineral	Pb–Zn hydrothermal		Later carbonate
	Pyrite–quartz	Sulfide–quartz	
Pyrite	▬▬	▬▬	
Molybdenite	▬		
Chalcopyrite	▬		
Quartz	▬▬	▬▬	
Sphalerite	▬	▬▬	
Galena	▬	▬▬	
Calcite	▬▬	▬▬	▬▬
Fluorite	▬	▬	▬
Ore structure	disseminated, vein, massive	disseminated, vein, massive, banded	disseminated
Ore texture	euhedral, subhedral, anhedral, metasomatic, cataclastic	euhedral, subhedral, anhedral, metasomatic, cataclastic, exsolution	euhedral, subhedral, anhedral

Fig. 4. Paragenetic sequence of minerals for the Shuikoushan Pb–Zn–Au ore district, South China.

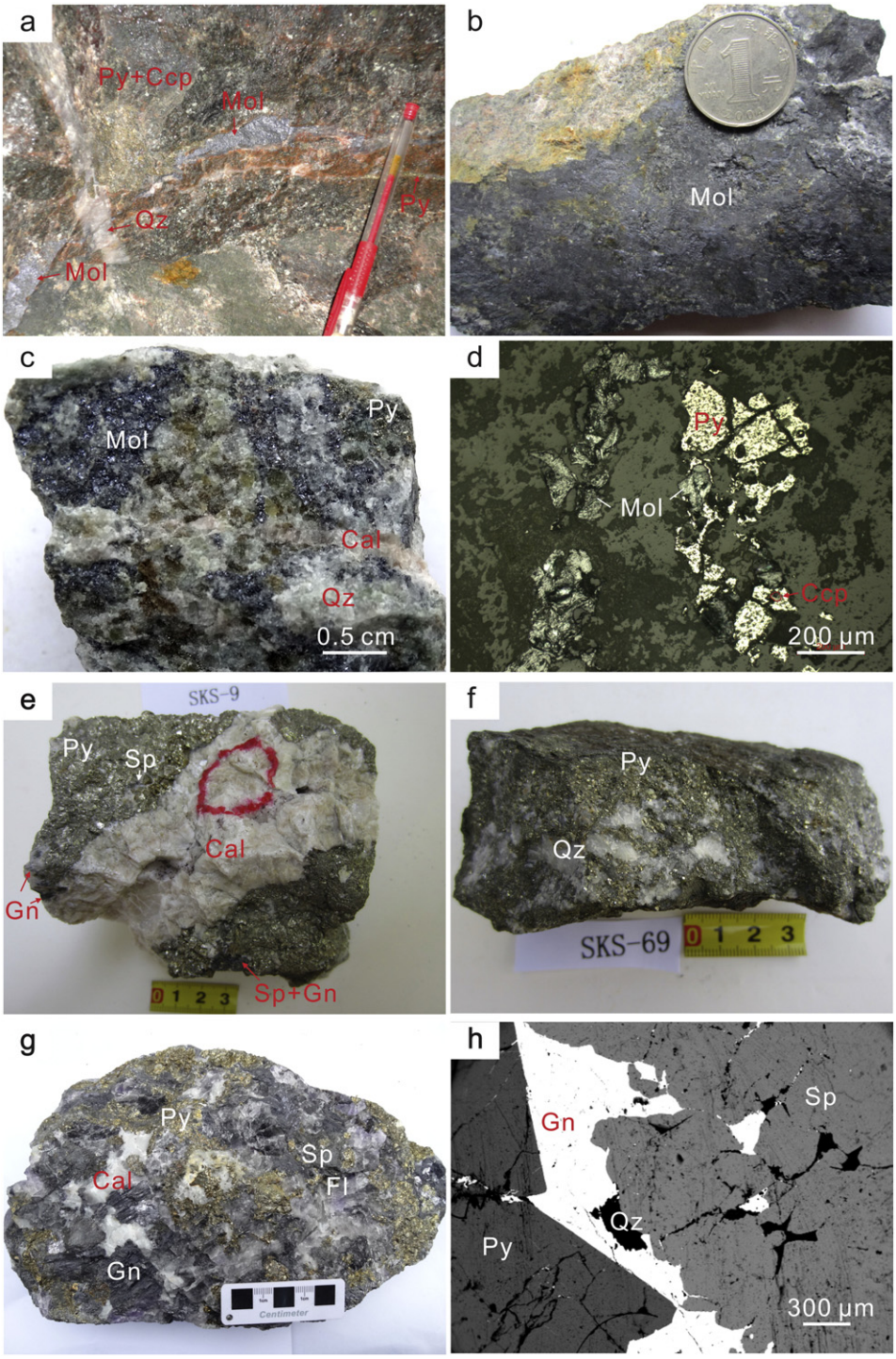

Fig. 5. Photographs of hand specimens and photomicrographs of ore and gangue minerals collected from the Shuikoushan Pb–Zn–Au ore district, South China. (a) Molybdenite vein associated with pyrite and minor chalcopyrite fill the fissures in the granodiorite intrusion. (b) Molybdenite vein. (c) Disseminated molybdenite associated with pyrite and quartz, cut by calcite veins. (d) Molybdenite associated with pyrite and chalcopyrite (under reflected light). (e) Massive pyrite associated with minor disseminated galena and sphalerite, cut by calcite vein. (f) Massive pyrite associated with quartz. (g) Brownish sphalerite coeval with galena, pyrite, calcite and minor fluorite. (h) Subhedral pyrite coeval with sphalerite and galena, and some sphalerite and galena veinlets replaced pyrite. Abbreviations: Cal — calcite; Ccp — chalcopyrite; Fl — fluorite; Gn — galena; Mol — molybdenite; Py — pyrite; Qz — quartz; and Sp — sphalerite.

91500 were cast in epoxy mounts and then polished to expose half of the crystals. All zircons were documented with transmitted and reflected light photomicrographs and cathodoluminescence (CL) images to reveal their internal textures (Fig. 6), and the mount was vacuum-coated with high-purity gold prior to SIMS analysis.

Measurements of U, Th and Pb were conducted using the Cameca IMS-1280 SIMS at the Institute of Geology and Geophysics, Chinese Academy of Sciences (CAS), using operating and data processing procedures similar to those described by Li et al. (2009). An uncertainty of 1% (1 RSD) for $^{206}Pb/^{238}U$ measurements of the standard zircons was propagated to the unknowns (Li et al., 2010). Measured compositions were corrected for common Pb using the abundance of non-radiogenic ^{204}Pb. Corrections are sufficiently small to be insensitive to the choice of common-Pb composition, and an average present-day

Fig. 6. Representative cathodoluminescence (CL) images of zircon grains for the granodiorite intrusion from the Shuikoushan Pb–Zn–Au ore district, South China.

crustal composition is used for the common Pb (Stacey and Kramers, 1975). Uncertainties on individual analyses in the data table are reported at the 1σ level; mean ages for pooled $^{206}Pb/^{238}U$ (and $^{207}Pb/^{206}Pb$) analyses are quoted with 95% confidence interval. Concordia diagrams and weighted mean calculations were made using Isoplot/Ex ver_3.0 (Ludwig, 2003).

4.2. Molybdenite Re–Os dating

Seven fine-grained euhedral molybdenite samples, intergrown with pyrite, minor chalcopyrite and quartz, were collected from different underground exposures at a depth about 480 m mining-level in the Laoyachao mining district. All molybdenite filled in fissures in the altered granodiorite intrusion and occurred as veinlets (Fig. 5a, b), except that sample SKS-95 was disseminated in quartz veins within the granodiorite intrusion (Fig. 5c, d).

Molybdenite separates were carefully selected under a binocular microscope after crushed less than 80 mesh, and then grounded to less than 200 mesh using an agate mill. Re–Os isotope analyses were performed at the Re–Os Isotope Laboratory, National Research Center of Geoanalysis, Chinese Academy of Geological Sciences (CAGS). The analytical procedures are similar to those described by Du et al. (2004). The determination of Re and Os concentration and isotopic compositions was performed on the inductively coupled plasma mass spectrometer (TJA X-series ICP-MS). The molybdenite standard GBW04436 (JDC) used in this study gave a mean value of 139.8 ± 2.0 Ma, which coincides well with the certified age of 139.6 ± 3.8 Ma (Du et al., 2004).

Total procedure blanks are about 3.3–3.7 pg for Re and about 0.15–0.27 pg for Os, which are considerably lower than the Re and Os concentrations in the analyzed samples in this study. The molybdenite model ages were calculated by $t = [\ln(1 + {}^{187}Os/{}^{187}Re)]/\lambda$, where λ is the ^{187}Re decay constant of 1.666×10^{-11} $year^{-1}$ (Smoliar et al., 1996). The Re–Os isochron age was calculated with Isoplot/Ex ver_3.0 (Ludwig, 2003). Absolute uncertainties of Re–Os data are given at the 2σ level.

Table 1
SIMS zircon U–Pb isotopic data for the Laoyachao granodiorite intrusion from the Shuikoushan Pb–Zn–Au ore district, South China.

Sample spot	U	Th	Pb	Th/U	f_{206}	$^{207}Pb/^{206}Pb$		$^{207}Pb/^{235}U$		$^{206}Pb/^{238}U$		$^{207}Pb/^{206}Pb$		$^{207}Pb/^{235}U$		$^{206}Pb/^{238}U$	
	ppm				%	Ratio	±1σ	Ratio	±1σ	Ratio	±1σ	Age (Ma)	±1σ	Age (Ma)	±1σ	Age (Ma)	±1σ
SKS-36-1	282	95	8	0.34	0.27	0.0483	3.3	0.1623	3.7	0.0244	1.5	111.7	77	152.7	5.2	155.4	2.4
SKS-36-2	357	227	11	0.64	0.09	0.0468	2.8	0.1636	3.2	0.0253	1.5	40.0	66	153.8	4.6	161.3	2.4
SKS-36-3	400	227	12	0.57	0.12	0.0495	1.9	0.1725	2.5	0.0253	1.5	169.2	44	161.6	3.7	161.0	2.4
SKS-36-4	406	138	12	0.34	0.00	0.0509	2.0	0.1758	2.6	0.0251	1.6	235.1	46	164.4	3.9	159.5	2.5
SKS-36-5	439	141	12	0.32	0.00	0.0499	1.9	0.1694	2.4	0.0246	1.5	188.2	43	158.9	3.5	157.0	2.4
SKS-36-6	365	224	11	0.61	0.08	0.0499	2.2	0.1732	2.7	0.0251	1.5	192.3	50	162.2	4.0	160.1	2.4
SKS-36-7	496	371	16	0.75	0.06	0.0489	1.7	0.1643	2.3	0.0244	1.5	144.1	39	154.4	3.3	155.1	2.4
SKS-36-8	1019	544	31	0.53	0.03	0.0496	2.4	0.1703	2.9	0.0249	1.5	175.4	56	159.7	4.2	158.7	2.4
SKS-36-9	504	308	16	0.61	0.00	0.0493	1.7	0.1696	2.3	0.0250	1.6	161.6	39	159.1	3.4	158.9	2.5
SKS-36-10	432	160	12	0.37	0.07	0.0493	2.1	0.1677	2.6	0.0247	1.5	161.0	48	157.4	3.8	157.2	2.4
SKS-36-11	465	276	15	0.59	0.00	0.0484	2.3	0.1669	2.7	0.0250	1.6	119.7	52	156.7	4.0	159.2	2.5
SKS-36-12	346	192	11	0.55	0.09	0.0501	2.3	0.1716	2.8	0.0248	1.6	199.5	52	160.8	4.1	158.2	2.4
SKS-36-13	356	104	10	0.29	0.09	0.0480	2.1	0.1684	2.7	0.0254	1.8	101.4	49	158.0	4.0	161.8	2.8
SKS-36-14	384	157	12	0.41	0.00	0.0488	1.9	0.1736	2.5	0.0258	1.6	136.5	44	162.6	3.7	164.4	2.6
SKS-36-15	237	103	7	0.43	0.00	0.0497	2.9	0.1686	3.3	0.0246	1.5	182.0	67	158.2	4.8	156.6	2.4
SKS-36-16	543	223	16	0.41	0.09	0.0494	1.6	0.1705	2.2	0.0250	1.6	167.0	37	159.9	3.3	159.4	2.5
SKS-36-17	432	186	13	0.43	0.12	0.0498	2.6	0.1683	3.0	0.0245	1.5	186.9	59	158.0	4.4	156.0	2.4
SKS-36-18	723	477	23	0.66	0.10	0.0499	1.6	0.1713	2.2	0.0249	1.5	188.4	37	160.6	3.3	158.7	2.4
SKS-36-19	341	172	11	0.51	0.10	0.0495	2.0	0.1754	2.8	0.0257	2.0	169.3	46	164.1	4.3	163.8	3.3

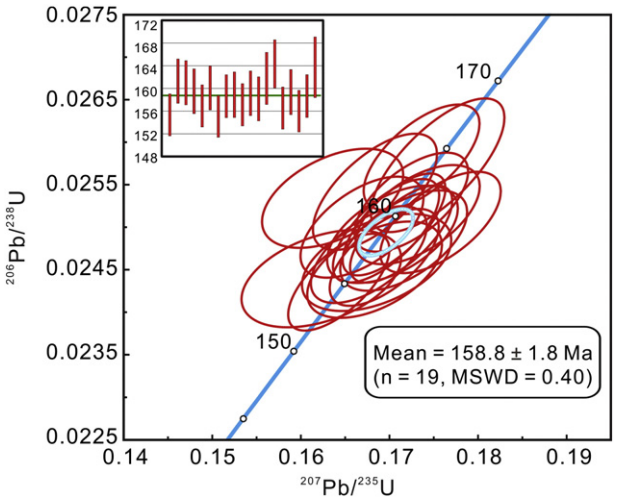

Fig. 7. Zircon U–Pb concordia diagram for the Shuikoushan Pb–Zn–Au ore district, South China.

Table 2
Re and Os isotopic data for molybdenite from the Shuikoushan Pb–Zn–Au ore district, South China.

Sample	Weight (mg)	Re(±2σ) (ppm)	^{187}Re(±2σ) (ppm)	^{187}Os(±2σ) (ppb)	Age(±2σ) (Ma)
SKS-95	1.03	1638 ± 13	1029 ± 8	2748 ± 21	160.0 ± 2.2
SKS-108	1.15	1841 ± 22	1157 ± 14	3051 ± 20	158.0 ± 2.6
SKS-109	1.33	1757 ± 22	1104 ± 14	2907 ± 18	157.8 ± 2.7
SKS-110	1.38	1319 ± 18	829.0 ± 11.1	2202 ± 13	159.2 ± 2.8
SKS-111	2.16	419.9 ± 3.7	263.9 ± 2.3	709 ± 4	161.0 ± 2.4
SKS-112	1.28	948.9 ± 9.9	596.4 ± 6.2	1567 ± 10	157.5 ± 2.5
SKS-113	1.15	705.4 ± 5.6	443.3 ± 3.5	1183 ± 7	160.0 ± 2.2

Uncertainty for the calculated ages is 0.57% at the 95% confidence level.

5. Analytical results

5.1. SIMS U–Pb age of zircon

Most zircons are euhedral, transparent, colorless and about 70–341 μm in length with aspect ratios between 1:1 and 5:1. Euhedral magmatic-origin oscillatory zoning is common in most zircon grains under CL (Fig. 6). Noticeably, no inherited cores were observed in zircons. Nineteen analyses of 19 zircon grains were obtained from the sample SKS-36 (Table 1). Their U and Th concentrations vary from 237 to 1019 ppm and 95 to 544 ppm, respectively, and Th/U ratios vary from 0.23 to 2.69. Common Pb is very low with f_{206} values <0.27%. All nineteen analyses are concordant in ^{206}Pb/^{238}U and ^{207}Pb/^{235}U within analytical errors (Fig. 7), yielding a well-defined concordia age of 158.8 ± 1.1 Ma (MSWD = 0.16, 95% confidence interval). This date coincides well with the weighted mean ^{206}Pb/^{238}U age of 158.8 ± 1.8 Ma (MSWD = 0.40).

5.2. Re–Os age of molybdenite

The Re–Os isotopic compositions of seven molybdenite separates are listed in Table 2 and illustrated in Fig. 8. These samples display relatively high Re concentrations, ranging from 420 to 1157 ppm. All analyzed samples in this study yield a narrow range of model ages from 157.5 ± 2.5 to 161.0 ± 2.4 Ma, with a weighted average age of 159.2 ± 0.91 Ma (MSWD = 1.2) (Fig. 8b). All analyzed samples give a well-defined ^{187}Re/^{187}Os isochron with an age of 157.8 ± 1.4 Ma (MSWD = 1.3) (Fig. 8a). A zero-intercept reveals that the molybdenite contains no detectable common ^{187}Os and that all ^{187}Os are radiogenic, which indicates that the model ages are reliable (Luck and Allègre, 1982; Selby and Creaser, 2001; Suzuki et al., 1996). The isochron age coincides well with the weighted average age within error, also reflecting that the molybdenite Re–Os dating is accurate.

6. Discussion

6.1. Emplacement age of the Shuikoushan pluton

Previous studies have attempted to determine the emplacement age of the granodiorite intrusion in the Shuikoushan ore district (Jin, 1989; Ma et al., 2006; Wang et al., 2002; Yu and Liu, 1997; Zuo et al., 2014), and acquired a wide range of ages (143–172 Ma). The whole-rock Rb–Sr and biotite K–Ar ages available for the studied granodiorite fall in a range of 143–160.7 Ma (Jin, 1989; Yu and Liu, 1997). Wang et al. (2002) first reported the U–Pb age of 172.3 ± 1.6 Ma using the isotope dilution (ID) method on single-grained zircon. Unfortunately, this date is obviously older than the newly-reported SHRIMP zircon U–Pb age (163 ± 2 Ma, Ma et al., 2006) and LA-ICP-MS zircon U–Pb age (156 ± 1 Ma; Zuo et al., 2014). Obviously, there is a wide variation for the granodiorite emplacement age by different dating methods, even the zircon U–Pb dating methods gave a wide range of 156–172.3 Ma. Therefore, a more accurate and precise emplacement age for the granodiorite intrusion is required for the Shuikoushan ore district.

The K–Ar and Rb–Sr systems are susceptible to disturbance or even complete resetting during alteration (Selby and Creaser, 2001; Stein et al., 2001; Suzuki et al., 1996), thus these K–Ar and Rb–Sr dates are not accurate. During the past several years, technical developments have provided opportunities for improved precision and accuracy,

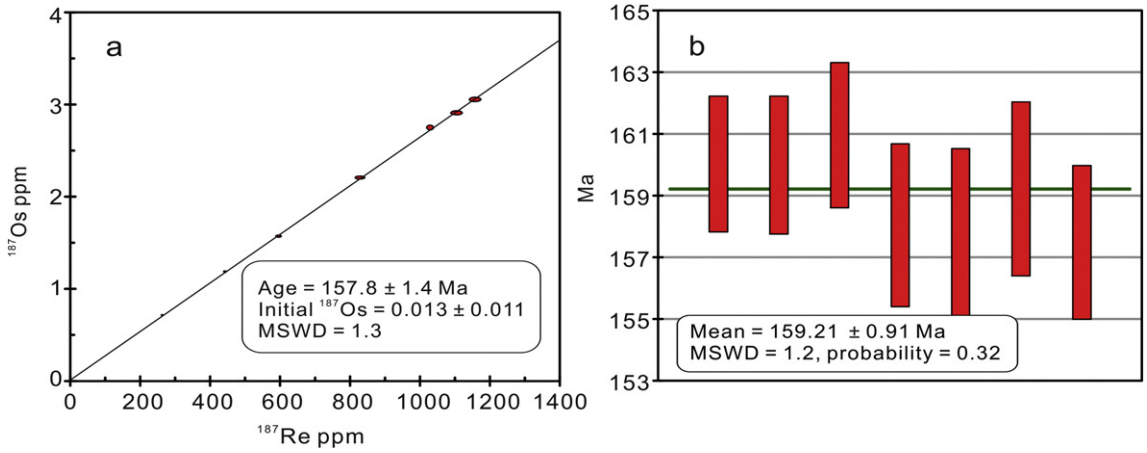

Fig. 8. Re–Os isochron diagram (a) and weighted average age diagram (b) for molybdenite separates from the Shuikoushan Pb–Zn–Au ore district, South China.

Table 3
Geochronological data available for Pb–Zn and W–Sn deposits and related granite in southern Hunan, South China.

		Metal association	Type of related intrusions	Age of mineralization				Age of related intrusion			
				Mineral	Method	Age (Ma)	Reference	Mineral	Method	Age (Ma)	Reference
I-type granite related	Shuikoushan	Pb–Zn–Au	Granodiorite	Mol	Re–Os	157.8 ± 1.4	This study	Zrn	SIMS U–Pb	158.8 ± 1.1	This study
								Zrn	LA–ICP-MS U–Pb	156.0 ± 1.0	Zuo et al. (2014)
								Zrn	SHRIMP U–Pb	163 ± 2	Ma et al. (2006)
								Zrn	ID U–Pb	172.3 ± 1.6	Wang et al. (2002)
	Baoshan	Pb–Zn–Cu	Granodiorite	Mol	Re–Os	160 ± 2	Lu et al. (2006)	Zrn	LA–ICP-MS U–Pb	157.7 ± 1.1	Xie et al. (2013)
								Zrn	LA–ICP-MS U–Pb	156.7 ± 1.4	Xie et al. (2013)
								Zrn	SHRIMP U–Pb	158 ± 2	Lu et al. (2006)
								Zrn	SHRIMP U–Pb	162.2 ± 1.6	Wu et al. (2005)
								Zrn	ID U–Pb	173.3 ± 1.9	Wang et al. (2002)
	Tongshanling	Pb–Zn–Cu	Granodiorite	Mol	Re–Os	162.2 ± 1.6	Yuan (2013)	Zrn	LA–MC–ICP-MS U–Pb	159.7 ± 0.8	Yuan and Wang (2013)
								Zrn	LA–MC–ICP-MS U–Pb	160.5 ± 0.9	Yuan, unpublished data
								Zrn	LA–MC–ICP-MS U–Pb	160.7 ± 0.5	Yuan, unpublished data
								Zrn	LA–ICP–MS U–Pb	166.6 ± 0.4	Quan et al. (2013)
								Zrn	SHRIMP U–Pb	163.6 ± 2.1	Jiang et al. (2009)
								Zrn	ID U–Pb	178.9 ± 1.7	Wang et al. (2002)
S-type granite related	Huangshaping	Pb–Zn–Cu–W–Mo	Quartz porphyry/ granite porphyry	Mol	Re–Os	159.4 ± 3.3	Lei et al. (2010)	Zrn	SHRIMP U–Pb	150 ± 3	Lei et al. (2010)
				Mol	Re–Os	157.5 ± 2.4	Lei et al. (2010)	Zrn	LA–ICP-MS U–Pb	161.6 ± 1.1	Yao et al. (2005)
				Mol	Re–Os	157.6 ± 2.3	Lei et al. (2010)				
				Mol	Re–Os	154.8 ± 1.9	Yao et al. (2007)				
				Mol	Re–Os	153.8 ± 4.8	Ma et al. (2007)				
	Yaogangxian	W	Granite	Mol	Re–Os	154.9 ± 2.6	Peng et al. (2006)	Zrn	SHRIMP U–Pb	155.4 ± 2.2	Li et al. (2011)
				Phl	Ar–Ar	153 ± 1.1	Peng et al. (2006)	Zrn	SHRIMP U–Pb	157.6 ± 2.6	Li et al. (2011)
				Bt	Ar–Ar	155.1 ± 1.1	Peng et al. (2006)	Zrn	SHRIMP U–Pb	158.4 ± 2.1	Li et al. (2011)
	Furong–Bailashui	Sn	Granite	Cst	U–Pb	159.9 ± 1.9	Yuan et al. (2011)	Zrn	SHRIMP U–Pb	156 ± 5	Li et al. (2006)

			Phl	Ar–Ar	150.6 ± 1.0	Peng et al. (2007)	Zrn	SHRIMP U–Pb	155 ± 6	Li et al. (2006)
			Phl	Ar–Ar	157.3 ± 1.0	Peng et al. (2007)	Bt	Ar–Ar	155.1 ± 1.8	Bai et al. (2005)
			Phl	Ar–Ar	154.7 ± 1.1	Peng et al. (2007)	Zrn	SHRIMP U–Pb	162 ± 2	Zhu et al. (2005)
			Hbl	Ar–Ar	156.9 ± 1.1	Peng et al. (2007)	Zrn	SHRIMP U–Pb	156.7 ± 1.7	Li et al. (2005)
Furong–Taoxiwo			Ms	Ar–Ar	159.9 ± 0.5	Peng et al. (2007)	Zrn	SHRIMP U–Pb	160 ± 2	Fu et al. (2004a)
			Ms	Ar–Ar	154.8 ± 0.6	Peng et al. (2007)				
			Ms	Ar–Ar	160.1 ± 0.9	Mao et al. (2004a)				
Furong–Shanmenkou			Ms	Ar–Ar	156.1 ± 0.4	Mao et al. (2004a)				
Xintianling	W	Granite	Ann	Ar–Ar	157.1 ± 0.2	Mao et al. (2004a)				
			Mol	Re–Os	161.7 ± 9.3	Yuan et al. (2012a)				
Jinchuantang	Sn–Bi	Granite	Mol	Re–Os	158.8 ± 6.6	Liu et al. (2012)	Zrn	SHRIMP U–Pb	152 ± 2	Li et al. (2004)
Hongqiling	Sn		Ms	Ar–Ar	153.6 ± 1.5	Yuan et al. (2012b)	Kfs	Ar–Ar	162.6 ± 3.3	Liu et al. (1997)
Shizhuyuan	W–Sn–Bi–Mo	Granite	Ms	Ar–Ar	148.2 ± 1.1	Peng et al. (2006)				
			Ms	Ar–Ar	153.4 ± 0.2	Mao et al. (2004b)				
			Mol	Re–Os	151.0 ± 3.5	Li et al. (1996)				
Xianghualing	Sn	Biotite granite	Cst	U–Pb	157 ± 6	Yuan et al. (2008)	Zrn	LA–MC–ICP-MS U–Pb	160.7 ± 2.2	Xuan et al. (2014)
			Ms	Ar–Ar	158.7 ± 1.2	Yuan et al. (2007)				
			Ms	Ar–Ar	154.4 ± 1.1	Yuan et al. (2007)				
Jiuyishan Da'ao	W–Sn	Granite	Mol	Re–Os	151.3 ± 2.4	Fu et al. (2007)	Zrn	SHRIMP U–Pb	156 ± 2	Fu et al. (2004b)
							Zrn	SHRIMP U–Pb	157 ± 1	Fu et al. (2004b)
Xitian	Sn	Granite	Mol	Re–Os (model age)	158.9 ± 2.2	Guo et al. (2014)	Zrn	SHRIMP U–Pb	228.5 ± 2.5	Ma et al. (2005)
			Mol	Re–Os (model age)	160.2 ± 3.2	Guo et al. (2014)	Zrn	SHRIMP U–Pb	155.5 ± 1.7	Ma et al. (2005)
			Mol	Re–Os	150 ± 2.7	Liu et al. (2008b)				
			Ms	Ar–Ar	155.6 ± 1.3	Ma et al. (2008)				
			Ms	Ar–Ar	157.2 ± 1.4	Ma et al. (2008)				
Hehuaping	Sn	Granite/granite porphyry	Mol	Re–Os	224.0 ± 1.9	Cai et al. (2006)	Zrn	LA–MC–ICP-MS U–Pb	235 ± 1.4	Zheng and Guo (2012)
							Zrn	LA–MC–ICP-MS U–Pb	155.9 ± 1.0	Zheng and Guo (2012)
							Zrn	SHRIMP U–Pb	212 ± 4	Cai et al. (2006)
							Zrn	LA–MC–ICP-MS U–Pb	154.7 ± 0.5	Zhang et al. (2010)
Jiepailing	Sn	Granite porphyry	Bt	Ar–Ar	91.1 ± 1.1	Mao et al. (2007)	Zrn	LA–MC–ICP-MS U–Pb	90.5 ± 0.9	Yuan et al. (2015)
			Ms	Ar–Ar	92.1 ± 0.7	Yuan et al. (2015)				

Abbreviations: Ann — annite; Bt — biotite; Cst — cassiterite; Hbl — hornblende; Kfs — K-feldspar; Mol — molybdenite; Ms — muscovite; Phl — phlogopite; and Zrn — zircon.

enhanced spatial resolution, and more efficient data acquisition using in-situ zircon U–Pb analysis (Gehrels et al., 2008; Gerdes and Zeh, 2006), especially the SIMS-based techniques can offer unparalleled spatial resolution for U–Pb age dating (usually 15 to 30 μm spot diameter and 2 to 5 μm penetration depth), thus, it is easy to observe and avoid the possible inclusions and fractures (Košler et al., 2002; Li et al., 2011) and it is the currently most widely accepted method for in situ U–Pb age determinations of zircon grains (Frei and Gerdes, 2009).

SIMS zircon U–Pb analysis carried out in this paper yields a weighted mean $^{206}Pb/^{238}U$ age of 158.8 ± 1.8 Ma (Fig. 7). This correlates well with the 163 ± 2 Ma age by Ma et al. (2006) and the 156 ± 1 Ma age of Zuo et al (2014). Therefore, the crystallization age of the granodiorite intrusion for Shuikoushan can be constrained at about 158 Ma.

6.2. Mineralization age of the Shuikoushan ore district

Molybdenite can provide robust Re–Os ages because it contains abundant Re and negligible initial or common Os (Markey et al., 1998; Selby and Creaser, 2001, 2004; Stein et al., 2001), and it is less sensitive to later hydrothermal, metamorphic, and/or tectonic events (e.g. Bingen and Stein, 2003; Selby and Creaser, 2001, 2004; Stein et al., 1998, 2001; Suzuki et al., 1996). Moreover, geologically younger, naturally fine-grained (<2 mm) molybdenite separates appear to display little $^{187}Re–^{187}Os$ decoupling and highly reproducible dates can be obtained using small quantities of samples (as little as 1 mg) (Selby and Creaser, 2004; Stein et al., 2001).

In this study, the fine-grained (mostly 0.1–1 mm) molybdenite separates used for Re–Os dating were well-homogenized into 200 mesh and have extremely high Re concentrations (420–1841 ppm), which reveals that $^{187}Re–^{187}Os$ decoupling effects in this study are negligible, thus the analyzed samples can yield accurate and precise molybdenite Re–Os ages (Selby and Creaser, 2004; Stein et al., 2001).

In addition, homogenization temperatures of fluid inclusions in sphalerite in the Laoyachao mining district vary in the range of 112.0–417.7 °C (Huang, unpublished data). These temperatures are lower than the Re–Os closure temperature for molybdenite, which is estimated to be about 500 °C (Suzuki et al., 1996). Therefore, the Re–Os isotopic system in molybdenite records the age of molybdenite crystallization.

In the Shuikoushan mining district, molybdenite formed during the Pb–Zn mineralization stage, therefore, the absolute timing for the lead and zinc mineralization in the mining district is estimated to be at about 158 Ma. This coincides with the geological relationship that some zinc mineralization fills in some fissures in the Early Jurassic sedimentary rocks, and orebodies are controlled by the Early Yanshanian (Jurassic) structures and occur along the contact zone between the granodiorite and sedimentary rocks (Liu and Tan, 1996).

6.3. Relationship between Pb–Zn mineralization and related intrusions

As mentioned above, the Pb–Zn mineralization in the Shuikoushan ore district is spatially associated with the Jurassic granodiorite. Moreover, the timing of Pb–Zn mineralization determined in this study (157.8 ± 1.4 Ma) coincides well with the emplacement of the Laoyachao granodiorite (158.8 ± 1.8 Ma). Thus, Pb–Zn mineralization and granodiorite emplacement in the district are closely associated temporally and spatially.

In addition, previous studies indicated that progressive Re contents transition from mantle-sourced, to mantle–crust mixing sourced, and then to crust-sourced origin (Mao et al., 1999; Stein et al., 2001). That is, those deposits with mantle inputs have significantly higher Re concentrations than those with crustal origin. In the Shuikoushan ore district, Re concentrations for molybdenite samples are extremely high (Table 1), varying from 420 to 1841 ppm, which are similar to the Re concentrations for molybdenite of mantle origin (>100 ppm, Mao et al., 1999; Stein et al., 2001), and slightly higher than the data (Re = 95–339 ppm) for the Baoshan Pb–Zn deposit (Lu et al., 2006), but significantly higher than the Re concentrations for W–Sn deposits in southern Hunan (e.g. Cai et al., 2006; Fu et al., 2007; Li et al., 1996; Liu et al., 2012; Peng et al., 2006; Yuan et al., 2012a). Thus, this indicates that major mantle substances were involved in the Shuikoushan mineralization.

In addition, the granodiorite intrusion in the Shuikoushan ore district is of I-type, with a crust–mantle mixed source (Huang et al., 2015; Wang et al., 2003). Therefore, there is evidence for a genetic relationship between the granodiorite intrusion and Pb–Zn mineralization. This can be further supported by the oxygen and hydrogen isotopic data for the Shuikoushan ore district, which reveal that the ore-forming fluids of the Shuikoushan ore district are of magmatic origin, although there is additional meteoric water in the later fluids (Liu, 1994). Consequently, the Shuikoushan Pb–Zn deposit is spatially, temporally and genetically related to the host granodiorite intrusions.

6.4. Implication for regional metallogeny

Based on previous limited geochronological data, Hua et al. (2005) and Mao et al. (2008, 2013) proposed that Pb–Zn mineralization in the Nanling Range was earlier than the W–Sn mineralization. Unfortunately, recent geochronological data available for Pb–Zn mineralization and the related intrusions in southern Hunan display about the same ages with the W–Sn mineralization. For comparison, this paper presents a compilation of the available geochronological data for the Mesozoic igneous rocks, associated Pb–Zn mineralization and W–Sn mineralization in southern Hunan as shown in Table 3 and Fig. 9, the latter is mainly based on Peng et al. (2008).

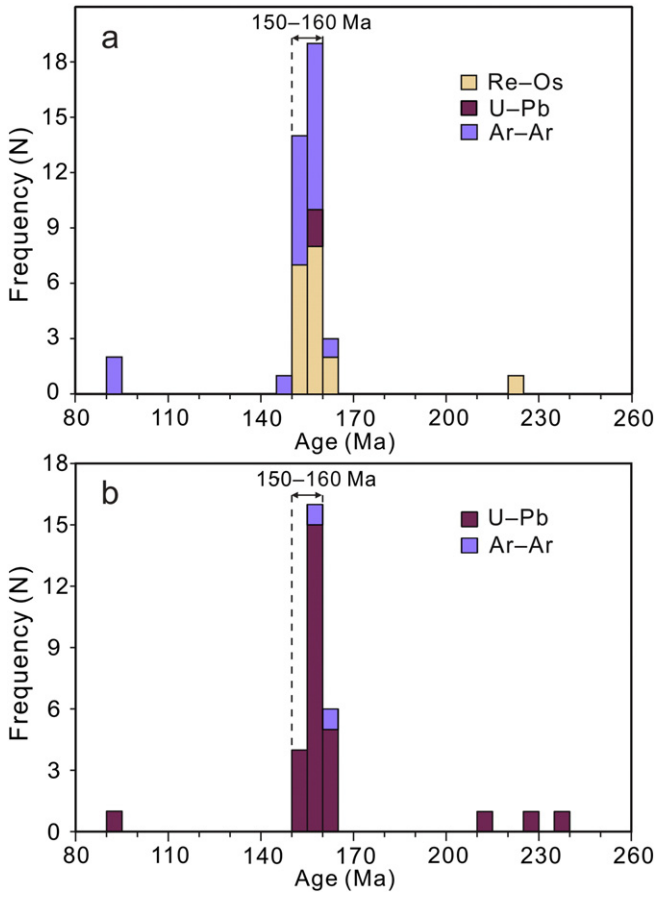

Fig. 9. Age histogram of W–Sn polymetallic deposits (a) and W–Sn-related granite (b) in southern Hunan.

In southern Hunan, the molybdenite Re–Os isochron age for the Baoshan deposit is 160 ± 2 Ma (Lu et al., 2006), which is coincident with the SHRIMP zircon U–Pb age of 158 ± 2 Ma (Lu et al., 2006) and LA–ICP-MS zircon U–Pb ages of 156.7 ± 1.4 Ma and 157.7 ± 1.1 Ma (Xie et al., 2013) for the granodiorite from the Baoshan deposit. Moreover, the Re–Os isochron age of molybdenite from the Yulong deposit in the Tongshanling ore district is 162.2 ± 1.6 Ma (Yuan, 2013), which is also consistent with the LA–ICP-MS zircon U–Pb ages of 159.7 ± 0.8 Ma, 160.5 ± 0.9 Ma and 160.7 ± 0.5 Ma for the granodiorite from the Tongshanling ore district (Yuan, unpublished data). As mentioned above, the Pb–Zn mineralization age for the Shuikoushan ore district from the molybdenite Re–Os isochron age (157.8 ± 1.4 Ma) in this paper also coincides well with the emplacement timing of the Laoyachao granodiorite (158.8 ± 1.8 Ma). Therefore, it can be concluded that the Pb–Zn mineralization in southern Hunan took place at about 160–156 Ma and there are no obvious time intervals between the magma emplacement and Pb–Zn mineralization in southern Hunan.

It has been generally accepted that the ore-forming metals, the ore-hosted layers, the lithologies of the ore-hosted rocks and the associated granitoids exhibit significant differences between the Pb–Zn deposits and the W–Sn deposits throughout the Nanling Range (Hua et al., 2003; Xu et al., 1982, 1983). However, the large-scale W–Sn mineralization in southern Hunan took place during 160–150 Ma as showed in Fig. 9a, which shares similar age range with the Pb–Zn mineralization in the area. Mao et al. (2007, 2013) suggested that the intense tectonic activity was caused by the NW-trending subduction of the Izanagi Plate beneath the Eurasian continent during the Jurassic. As the subduction of the Izanagi Plate continued, continental crust gradually thickened and developed a series of NE-trending lithospheric extensional belts and deep faults in a back-arc setting (Mao et al., 2007, 2008, 2013). A series of granite belts with low t_{DM} and high ε_{Nd} values (Shi-Hang Belt or Qin-Hang Belt) reported by Gilder et al. (1996), Chen and Jahn (1998) and Hong et al. (2002) exactly recorded the continental extension event. Consequently, abundant magmas emplaced in the Nanling Range and adjacent areas and caused large-scale W–Sn mineralization during 160–150 Ma under the lithospheric extensional tectonic regime. Therefore, just like W–Sn mineralization, the Pb–Zn mineralization was probably ascribed to a same lithosphere extensional event. However, it's still unclear why W–Sn mineralization and Pb–Zn mineralization formed at nearly coeval time, and the genetic associations between the W–Sn mineralization and Pb–Zn mineralization in the Nanling Range are needed to be ascertained.

7. Conclusions

Re–Os dating on molybdenite reveals that the Shuikoushan Pb–Zn deposit formed at 157.8 ± 1.4 Ma, coincident with the new SIMS zircon U–Pb age (158.8 ± 1.8 Ma) for the Shuikoushan granodiorite intrusion associated with the Pb–Zn mineralization, revealing a genetic link between the Pb–Zn hydrothermal mineralization and the granodiorite emplacement in the area.

Integrated with other highly precise geochronological data obtained previously, it is concluded that the regional Pb–Zn mineralization formed during 160–156 Ma in southern Hunan, rather than 180–170 Ma or 170–160 Ma as considered previously. The Pb–Zn mineralization and major W–Sn mineralization in southern Hunan took place at about the same time, suggesting that a common geological event is responsible for their genesis.

Conflict of interest

We have no conflicts of interest to declare.

Acknowledgments

This research was financially supported by the National Key Basic Research Program of China (973 Program, Grant No. 2012CB416705) and the National Natural Science Foundation of China (Grant Nos. 41303030, 41473043). We thank the geologists of the Shuikoushan Mine for their help during our field investigations. Special thanks are due to Prof. Li Xianhua for his help with the zircon U–Pb isotope analyses and Mr. Li Chao for his help with the rhenium and osmium isotope analyses. We are grateful to Prof. Franco Pirajno and Prof. Mao Jingwen and two anonymous reviewers for their constructive comments which have significantly improved the manuscript.

References

Bai, D.Y., Chen, J.C., Ma, T.Q., Wang, X.H., 2005. Geochemical characteristic and tectonic setting of Qitianling A-type granitic pluton in southern Hunan. Acta Petrol. Mineral. 24, 255–272 (in Chinese with English abstract).

Bingen, B., Stein, H., 2003. Molybdenite Re–Os dating of biotite dehydration melting in the Rogaland high-temperature granulites, S Norway. Earth Planet. Sci. Lett. 208, 181–195.

Cai, M.H., Chen, K.X., Qu, W.J., Liu, G.Q., Fu, J.M., Yin, J.P., 2006. Geological characteristics and Re–Os dating of molybdenites in Hehuaping tin–polymetallic deposit, southern Hunan Province. Mineral Deposits 25, 263–268 (in Chinese with English abstract).

Chen, J.F., Jahn, B.M., 1998. Crustal evolution of Southeastern China, Nd and Sr isotopic evidence. Tectonophysics 284, 101–133.

Du, A.D., Wu, S.Q., Sun, D.Z., Wang, S.X., Qu, W.J., Markey, R., Stain, H., Morgan, J., Malinovskiy, D., 2004. Preparation and certification of Re–Os dating reference materials: molybdenites HLP and JDC. Geostand. Geoanal. Res. 28, 41–52.

Feng, C.Y., Zeng, Z.L., Zhang, D.Q., Qu, W.J., Du, A.D., Li, D.X., She, H.Q., 2011. SHRIMP zircon U–Pb and molybdenite Re–Os isotopic dating of the tungsten deposits in the Tianmenshan–Hongtaoling W–Sn orefield, southern Jiangxi Province, China, and geological implications. Ore Geol. Rev. 43, 8–25.

Frei, D., Gerdes, A., 2009. Precise and accurate in-situ U–Pb dating of zircon with high sample throughput by automated LA–SF-ICP-MS. Chem. Geol. 261, 261–270.

Fu, J.M., Ma, C.Q., Xie, C.F., Zhang, Y.M., Peng, S.B., 2004a. Zircon SHRIMP dating of the Cailing granite on the eastern margin of the Qitianling granite, Hunan, South China, and its significance. Geol. China 31, 96–100 (in Chinese with English abstract).

Fu, J.M., Ma, C.Q., Xie, C.F., Zhang, Y.M., Peng, S.B., 2004b. SHRIMP U–Pb zircon dating of the Jiuyishan composite granite in Hunan and its geological significance. Geotecton. Metallog. 28, 370–378 (in Chinese with English abstract).

Fu, J.M., Ma, C.Q., Xie, C.F., Zhang, Y.M., Peng, S.B., 2005. Ascertainment of the Jinjiling aluminous A-type granite, Hunan Province and its tectonic settings. Geochimica 34, 215–226 (in Chinese with English abstract).

Fu, J.M., Li, H.Q., Qu, W.J., Yang, X.J., Wei, J.Q., Liu, G.Q., Ma, L.Y., 2007. Re–Os isotope dating of the Da'ao tungsten–tin deposit in the Jiuyi Mountains, southern Hunan Province. Geol. China 34, 651–656 (in Chinese with English abstract).

Gehrels, G.E., Valencia, V.A., Ruiz, J., 2008. Enhanced precision, accuracy, efficiency, and spatial resolution of U–Pb ages by laser ablation–multicollector–inductively coupled plasma-mass spectrometry. Geochem. Geophys. Geosyst. http://dx.doi.org/10.1029/2007GC001805.

Gerdes, A., Zeh, A., 2006. Combined U–Pb and Hf isotope LA–(MC–)ICP-MS analyses of detrital zircons: Comparison with SHRIMP and new constraints for the provenance and age of an Armorican metasediment in Central Germany. Earth Planet. Sci. Lett. 249, 47–61.

Gilder, S.A., Gill, J., Coe, R.S., Zhao, X.X., Liu, Z.W., Wang, G.X., Yuan, K.R., Liu, W.L., Kuang, G.D., Wu, H.R., 1996. Isotopic and paleomagnetic constraints on the Mesozoic tectonic evolution of south China. J. Geophys. Res. Solid Earth 101, 16137–16154.

Guo, C.L., Mao, J.W., Bierlein, F., Chen, Z.H., Chen, Y.C., Li, C.B., Zeng, Z.L., 2011. SHRIMP U–Pb (zircon), Ar–Ar (muscovite) and Re–Os (molybdenite) isotopic dating of the Taoxikeng tungsten deposit, South China Block. Ore Geol. Rev. 43, 26–39.

Guo, C.L., Li, C., Wu, S.C., Xu, Y.M., 2014. Molybdenite Re–Os isotopic dating of Xitian deposit in Hunan Province and its geological significance. Rock Miner. Anal. 33, 142–152 (in Chinese with English abstract).

Hong, D.W., Xie, X.L., Zhang, J.S., 2002. Geological significance of the Hangzhou–Zhuguangshan–Huashan high-ε_{Nd} granite belt. Geol. Bull. China 21, 348–354 (in Chinese with English abstract).

Hsu, K.C., 1943. Tungsten deposits of southern Kiangsi, China. Econ. Geol. 38, 431–474.

Hu, R.Z., Wei, W.F., Bi, X.W., Peng, J.T., Qi, Y.Q., Wu, L.Y., Chen, Y.W., 2012. Molybdenite Re–Os and muscovite $^{40}Ar/^{39}Ar$ dating of the Xihuashan tungsten deposit, central Nanling district, South China. Lithos 150, 111–118.

Hua, R.M., Chen, P.R., Zhang, W.L., Liu, X.D., Lu, J.J., Lin, J.F., Yao, J.M., Qi, H.W., Zhang, Z.S., Gu, S.Y., 2003. Metallogenic systems related to Mesozoic and Cenozoic granitoids in South China. Sci. China, Ser. D 46, 816–829.

Hua, R.M., Chen, P.R., Zhang, W.L., Lu, J.J., 2005. Three major metallogenic events in Mesozoic in South China. Mineral Deposits 24, 99–107 (in Chinese with English abstract).

Huang, J.C., Peng, J.T., Yang, J.H., Xu, C.X., Hu, S.B., 2015. Geochemistry and genesis of the Shuikoushan granodiorite, southern Hunan, South China. Geochimica 44, 131–144 (in Chinese with English abstract).

IGCAS (Institute of Geochemistry, Chinese Academy of Sciences), 1979. Geochemistry of Granitoids in Southern China. Science Publishing House, Beijing, pp. 1–421 (in Chinese).

Jiang, S.Y., Zhao, K.D., Jiang, Y.H., Ling, H.F., Ni, P., 2006. New type of tin mineralization related to granite in South China: evidence from mineral chemistry, element and isotope geochemistry. Acta Petrol. Sin. 22, 2509–2516 (in Chinese with English abstract).

Jiang, S.Y., Zhao, K.D., Jiang, Y.H., Dai, B.Z., 2008. Characteristics and genesis of Mesozoic A-type granites and associated mineral deposits in the southern Hunan and northern Guangxi provinces along the Shi-Hang Belt, South China. Geol. J. China Univ. 14, 496–509 (in Chinese with English abstract).

Jiang, Y.H., Jiang, S.Y., Dai, B.Z., Liao, S.Y., Zhao, K.D., Ling, H.F., 2009. Middle to late Jurassic felsic and mafic magmatism in southern Hunan Province, southeast China: implications for a continental arc to rifting. Lithos 107, 185–204.

Jin, R.L., 1989. A tentative approach to the genetic types and controlling factors of silver deposits in Hunan. J. Guilin College Geol. 9, 139–146 (in Chinese with English abstract).

Košler, J., Fonneland, H., Sylvester, P., Tubrett, M., Pedersen, R.B., 2002. U–Pb dating of detrital zircons for sediment provenance studies — a comparison of laser ablation ICPMS and SIMS techniques. Chem. Geol. 182, 605–618.

Lei, Z.H., Chen, F.W., Chen, Z.H., Xu, Y.M., Gong, S.Q., Li, H.Q., Mei, Y.P., Qu, W.J., Wang, D.H., 2010. Petrogenetic and metallogenic age determination of the Huangshaping lead–zinc polymetallic deposit and its geological significance. Acta Geosci. Sin. 31, 532–541 (in Chinese with English abstract).

Li, N.Q., Peng, C., 1996. Shuikoushan Lead–Zinc–Gold–Silver Orefield, Hunan, China. Seismological Publishing House, Beijing, pp. 1–103 (in Chinese).

Li, H.Y., Mao, J.W., Sun, Y.L., Zou, X.Q., He, H.L., Du, A.D., 1996. Re–Os isotopic chronology of molybdenites in the Shizhuyuan polymetallic tungsten deposit, southern Hunan. Geol. Rev. 42, 261–267 (in Chinese with English abstract).

Li, X.H., Liu, D.Y., Sun, M., LI, W.X., Liang, X.R., Liu, Y., 2004. Precise Sm–Nd and U–Pb isotopic dating of the supergiant Shizhuyuan polymetallic deposit and its host granite, SE China. Geol. Mag. 141, 225–231.

Li, J.D., Bai, D.Y., Wu, G.Y., Che, Q.J., Liu, Y.R., Ma, T.Q., 2005. Ziron SHRIMP dating of the Qitianling granite, Chenzhou, southern Hunan, and its geological significance. Geol. Bull. China 24, 411–414 (in Chinese with English abstract).

Li, H.Q., Lu, Y.F., Wang, D.H., Chen, Y.C., Yang, H.M., Guo, J., Xie, C.F., Mei, Y.P., Ma, L.Y., 2006. Dating of the rock-forming and ore-forming ages and their geological significances in the Furong ore-field, Qitian Mountain, Hunan. Geol. Rev. 52, 113–121 (in Chinese with English abstract).

Li, X.H., Li, Z.X., Li, W.X., Liu, Y., Yuan, C., Wei, G.J., Qi, C.S., 2007a. U–Pb zircon, geochemical and Sr–Nd–Hf isotopic constraints on age and origin of Jurassic I- and A-type granites from central Guangdong, SE China: a major igneous event in response to foundering of a subducted flat-slab? Lithos 96, 186–204.

Li, Z.L., Hu, R.Z., Yang, J.S., Peng, J.T., Li, X.M., Bi, X.W., 2007b. He, Pb and S isotopic constraints on the relationship between the A-type Qitianling granite and the Furong tin deposit, Hunan Province, China. Lithos 97, 161–173.

Li, X.H., Liu, Y., Li, Q.L., Guo, C.H., Chamberlain, K.R., 2009. Precise determination of Phanerozoic zircon Pb/Pb age by multicollector SIMS without external standardization. Geochem. Geophys. Geosyst. http://dx.doi.org/10.1029/2009GC002400.

Li, Q.L., Li, X.H., Liu, Y., Tang, G.Q., Yang, J.H., Zhu, W.G., 2010. Precise U–Pb and Pb–Pb dating of Phanerozoic baddeleyite by SIMS with oxygen flooding technique. J. Anal. At. Spectrom. 25, 1107–1113.

Li, S.T., Wang, J.B., Zhu, X.Y., Wang, Y.L., Han, Y., Guo, N.N., 2011. Chronological characteristics of the Yaogangxian composite pluton in Hunan Province. Geol. Prospect. 47, 143–150 (in Chinese with English abstract).

Liu, Z.Q., 1980. Theory of the Metallogenic Prediction for the Vein Type Tungsten Deposits. Science Publishing House, Beijing, pp. 1–150 (in Chinese).

Liu, W., 1994. Nature, source and convection path of the ore-bearing fluid in the Shuikoushan Pb–Zn–Au ore field. Geotecton. Metallog. 18, 209–218 (in Chinese).

Liu, S.S., Tan, K.X., 1996. Dynamics of tectonic ore-forming in open system in Shuikoushan ore field, Hunan. Geotecton. Metallog. 20, 1–9 (in Chinese with English abstract).

Liu, Y.M., Dai, T.M., Lu, H.Z., Xu, Y.Z., Wang, C.L., Kang, W.Q., 1997. Isotopic date of $^{40}Ar/^{39}Ar$ and Sm–Nd for diagenesis–metallogenesis of the Qianlishan granite. Sci. China, Ser. D 27, 425–430 (in Chinese).

Liu, S.B., Wang, D.H., Chen, Y.C., Li, J.K., Ying, L.J., Xu, J.X., Zeng, Z.L., 2008a. $^{40}Ar/^{39}Ar$ ages of muscovite from different types tungsten-bearing quartz veins in the Chong-Yu-You concentrated mineral area in Gannan region and its geological significance. Acta Geol. Sin. 82, 932–940 (in Chinese with English abstract).

Liu, G.Q., Wu, S.C., Du, A.D., Fu, J.M., Yang, X.J., Tang, Z.H., Wei, J.Q., 2008b. Metallogenic ages of the Xitian tungsten–tin deposit, eastern Hunan Province. Geotecton. Metallog. 32, 63–71 (in Chinese with English abstract).

Liu, X.F., Yuan, S.D., Wu, S.H., 2012. Re–Os dating of the molybdenite from the Jinchuantang tin–bismuth deposit in Hunan Province and its geological significance. Acta Petrol. Sin. 28, 39–51 (in Chinese with English abstract).

Lu, H.Z., 1986. Origin of Tungsten Mineral Deposit in South China. Publishing House of Chongqing, Chongqing, pp. 1–232 (in Chinese with English abstract).

Lu, Y.F., Ma, L.Y., Qu, W.J., Mei, Y.P., Chen, X.Q., 2006. U–Pb and Re–Os isotope geochronology of Baoshan Cu–Mo polymetallic ore deposit in Hunan Province. Acta Petrol. Sin. 22, 2483–2492 (in Chinese with English abstract).

Lu, R., Xu, Z.W., Lu, J.J., Wang, R.C., Zuo, C.H., Zhao, Z.X., Miao, B.H., 2013. Genesis of the Shuikoushan lead–zinc deposit, Changning City, Hunan Province. J. Nanjing Univ. (Nat. Sci.) 49, 732–746 (in Chinese with English abstract).

Luck, J.M., Allègre, C.J., 1982. The study of molybdenites through the $^{187}Re–^{187}Os$ chronometer. Earth Planet. Sci. Lett. 61, 291–296.

Ludwig, K.R., 2003. ISOPLOT 3.00: A Geochronological Toolkit for Microsoft Excel. Berkeley Geochronology Center, Berkeley, California.

Ma, T.Q., Bai, D.Y., Kuang, J., Wang, X.H., 2005. Zircon SHRIMP dating of the Xitian granite pluton, Chaling, southeastern Hunan, and its geological significance. Geol. Bull. China 24, 415–419 (in Chinese with English abstract).

Ma, L.Y., Lu, Y.F., Mei, Y.P., Chen, X.Q., 2006. Zircon SHRIMP U–Pb dating of granodiorite from Shuikoushan ore-field, Hunan Province and its geological significance. Acta Petrol. Sin. 22, 2475–2482 (in Chinese with English abstract).

Ma, L.Y., Lu, Y.F., Qu, W.J., Fu, J.M., 2007. Re–Os isotopic chronology of molybdenites in Huangshaping lead–zinc deposit, southeast Hunan, and its geological implications. Mineral Deposits 26, 425–431 (in Chinese with English abstract).

Ma, L.Y., Fu, J.M., Wu, S.C., Xu, D.M., Yang, X.J., 2008. $^{40}Ar/^{39}Ar$ isotopic dating of the Longshang tin–polymetallic deposit, Xitian orefield, eastern Hunan. Geol. China 35, 706–713 (in Chinese with English abstract).

Mao, J.W., Li, H.Y., 1995. Evolution of the Qianlishan granite stock and its relation to the Shizhuyuan polymetallic tungsten deposit. Int. Geol. Rev. 37, 63–80.

Mao, J.W., Li, H.Y., 1996. Geology and metallogeny of the Shizhuyuan skarn–greisen deposit, Hunan Province, China. Int. Geol. Rev. 38, 1020–1039.

Mao, J.W., Li, H.Y., Song, X.X., Rui, B., Xu, Y.Z., Wang, D.H., Lan, X.M., Zhang, J.K., 1998. Geology and Geochemistry of the Shizhuyuan W–Sn–Mo–Bi Polymetallic Deposit, Hunan Province. Geological Publishing House, Beijing, pp. 1–215 (in Chinese).

Mao, J.W., Zhang, Z.C., Zhang, Z.H., Du, A.D., 1999. Re–Os isotopic dating of molybdenites in the Xiaoliugou W (Mo) deposit in the Northern Qilian Mountains and its geological significance. Geochim. Cosmochim. Acta 63, 1815–1818.

Mao, J.W., Li, X.F., Lehmann, B., Chen, W., Lan, X.M., Wei, S.L., 2004a. $^{40}Ar–^{39}Ar$ dating of tin ores and related granite in Furong tin orefield, Hunan Province, and its geodynamic significance. Mineral Deposits 23, 164–175 (in Chinese with English abstract).

Mao, J.W., Xie, G.Q., Li, X.F., Zhang, C.Q., Mei, Y.X., 2004b. Mesozoic large scale mineralization and multiple lithospheric extension in South China. Earth Sci. Front. 11, 45–55 (in Chinese with English abstract).

Mao, J.W., Xie, G.Q., Guo, C.L., Chen, Y.C., 2007. Large-scale tungsten–tin mineralization in the Nanling region, South China: metallogenic ages and corresponding geodynamic processes. Acta Petrol. Sin. 23, 2329–2338 (in Chinese with English abstract).

Mao, J.W., Xie, G.Q., Guo, C.L., Yuan, S.D., Cheng, Y.B., Chen, Y.C., 2008. Spatial–temporal distribution of Mesozoic ore deposits in South China and their metallogenic settings. Geol. J. China Univ. 14, 510–526 (in Chinese with English abstract).

Mao, J.W., Cheng, Y.B., Chen, M.H., Franco, P., 2013. Major types and time–space distribution of Mesozoic ore deposits in South China and their geodynamic settings. Miner. Deposita 48, 267–294.

Markey, R., Stein, H., Morgan, J., 1998. Highly precise Re–Os dating for molybdenite using alkaline fusion and NTIMS. Talanta 45, 935–946.

Mo, Z.S., Li, H.M., Kang, Y.F., 1958. Preliminary Summary Industrial Type and Exploration Methods for the Tungsten Deposits in South China. Geological Publishing House, Beijing, pp. 1–103 (in Chinese).

Mo, Z.S., Ye, B.D., Pan, W.Z., Wan, S.N., 1980. Geology of Granites in Nanling Range. Geological Publishing House, Beijing, pp. 1–363 (in Chinese).

Peng, J.T., Zhou, M.F., Hu, R.Z., Shen, N.P., Yuan, S.D., Bi, X.W., Du, A.D., Qu, W.J., 2006. Precise molybdenite Re–Os and mica Ar–Ar dating of the mesozoic Yaogangxian tungsten deposit, central Nanling district, South China. Miner. Deposita 41, 661–669.

Peng, J.T., Hu, R.Z., Bi, X.W., Dai, T.M., Li, Z.L., Li, X.M., Shuang, Y., Yuan, S.D., Liu, S.R., 2007. $^{40}Ar/^{39}Ar$ isotopic dating of tin mineralization in Furong deposit of Hunan Province and its geological significance. Mineral Deposits 26, 237–248 (in Chinese with English abstract).

Peng, J.T., Hu, R.Z., Yuan, S.D., Bi, X.W., Shen, N.P., 2008. The time ranges of granitoid emplacement and related nonferrous metallic mineralization in southern Hunan. Geol. Rev. 54, 617–625 (in Chinese with English abstract).

Qi, H.W., Hu, R.Z., Wang, X.F., Qu, W.J., Bi, X.W., Peng, J.T., 2012. Molybdenite Re–Os and muscovite $^{40}Ar/^{39}Ar$ dating of quartz vein-type W–Sn polymetallic deposits in northern Guangdong, South China. Miner. Deposita 47, 607–622.

Quan, T.J., Wang, G., Zhong, J.L., Fei, L.D., Kong, H., Liu, S.J., Zhao, Z.Q., Guo, B.Y., 2013. Petrogenesis of granodiorites in Tongshanling deposit of Hunan Province: constraints from petrogeochemistry, zircon U–Pb chronology and Hf isotope. J. Mineral. Petrol. 33, 43–52 (in Chinese with English abstract).

RGNTD (Research Group for Nanling Tungsten Deposits, Chinese Ministry of Metallurgy), 1985. Tungsten Deposit in South China. Metallurgy Industry Press, Beijing, pp. 1–496 (in Chinese).

Selby, D., Creaser, R.A., 2001. Re–Os geochronology and systematics in molybdenite from the Endako porphyry molybdenum deposit, British Columbia, Canada. Econ. Geol. 96, 197–204.

Selby, D., Creaser, R.A., 2004. Macroscale NTIMS and microscale LA–MC–ICP-MS Re–Os isotopic analysis of molybdenite: testing spatial restrictions for reliable Re–Os age determinations, and implications for the decoupling of Re and Os within molybdenite. Geochim. Cosmochim. Acta 68, 3897–3908.

Smoliar, M.I., Walker, R.J., Morgan, J.W., 1996. Re–Os ages of group IIA, IIIA, IVA, and IVB iron meteorites. Science 271, 1099–1102.

Stacey, J.S., Kramers, J.D., 1975. Approximation of terrestrial lead isotope evolution by a two-stage model. Earth Planet. Sci. Lett. 26, 207–221.

Stein, H.J., Sundblad, K., Markey, R.J., Morgan, J.W., Motuza, G., 1998. Re–Os ages for Archean molybdenite and pyrite, Kuittila-Kivisuo, Finland and Proterozoic molybdenite, Kabeliai, Lithuania: testing the chronometer in a metamorphic and metasomatic setting. Miner. Deposita 33, 329–345.

Stein, H.J., Markey, R.J., Morgan, J.W., Hannah, J.L., Scherstén, A., 2001. The remarkable Re–Os chronometer in molybdenite: how and why it works. Terra Nova 13, 479–486.

Suzuki, K., Shimizu, H., Masuda, A., 1996. Re–Os dating of molybdenites from ore deposits in Japan: implication for the closure temperature of the Re–Os system for molybdenite and the cooling history of molybdenum ore deposits. Geochim. Cosmochim. Acta 60, 3151–3159.

Tan, J.X., Wan, K.Y., 2008. Geochemical characteristics of the Shuikoushan Pb–Zn–Au–Ag deposit, Hunan. Miner. Resour. Geol. 22, 125–130 (in Chinese with English abstract).

Wang, C.L., Luo, S.W., Xu, Y.Z., Sun, Y.H., Xie, C.G., Zhang, C.M., 1987. Geology of the Shizhuyuan Tungsten Polymetallic Deposits. Geological Publishing House, Beijing, pp. 1–147 (in Chinese).
Wang, Y.M., Zhu, J.A., Yu, Q.H., 1988. Geology of Pb–Zn Deposits, Hunan Province, China. Geological Publishing House, Beijing, pp. 1–419 (in Chinese).
Wang, Y.J., Fan, W.M., Guo, F., Li, H.M., Liang, X.Q., 2002. U–Pb dating of early Mesozoic granodioritic intrusions in southeastern Hunan Province, South China and its petrogenetic implications. Sci. China, Ser. D 45, 280–288.
Wang, Y.J., Fan, W.M., Guo, F., 2003. Geochemistry of early Mesozoic potassium-rich diorites–granodiorites in southeastern Hunan Province, South China: petrogenesis and tectonic implications. Geochem. J. 37, 427–448.
Wang, D.H., Chen, Y.C., Chen, W., 2004. Dating the Dachang giant tin polymetallic deposit in Nandan, Guangxi. Acta Geol. Sin. 78, 132–138 (in Chinese with English abstract).
Wu, G.Y., Ma, T.Q., Bai, D.Y., Li, J.D., Che, Q.J., Wang, X.H., 2005. Petrological and geochemical characteristics of granodioritic cryptoexplosion breccia and zircon SHRIMP dating in the Baoshan area, Hunan Province. Geoscience 19, 198–204 (in Chinese with English abstract).
Xie, Y.C., Lu, J.J., Ma, D.S., Zhang, R.Q., Gao, J.F., Yao, Y., 2013. Origin of granodiorite porphyry and mafic microgranular enclave in the Baoshan Pb–Zn polymetallic deposit, southern Hunan Province: zircon U–Pb chronological, geochemical and Sr–Nd–Hf isotopic constraints. Acta Petrol. Sin. 29, 4186–4214 (in Chinese with English abstract).
Xu, K.Q., Ding, Y., 1938. Viewpoints on the genesis and classification for the tungsten deposits in China. Geol. Rev. 3, 305–325 (in Chinese).
Xu, K.Q., Hu, S.X., Sun, M.Z., Ye, J., 1982. On the two genetic series of granites in Southeastern China and their metallogenetic characteristics. Mineral Deposits 2, 1–14 (in Chinese with English abstract).
Xu, K.Q., Hu, S.X., Sun, M.Z., Zhang, J.R., Ye, J., 1983. On the genetic series of granites, as exemplified by the Mesozoic granites of South China. Acta Geol. Sin. 2, 107–118 (in Chinese with English abstract).
Xuan, Y.S., Yuan, S.D., Yuan, Y.B., Mi, J.R., 2014. Zircon U–Pb age, geochemistry and petrogenesis of Jianfengling pluton in southern Hunan Province. Mineral Deposits 33, 1379–1390 (in Chinese with English abstract).
Yao, J.M., Hua, R.M., Lin, J.F., 2005. Zircon LA–ICP-MS U–Pb dating and geochemical characteristics of Huangshaping granite in southeast Hunan Province, China. Acta Petrol. Sin. 21, 688–696 (in Chinese with English abstract).
Yao, J.M., Hua, R.M., Qu, W.J., Qi, H.W., Lin, J.F., Du, A.D., 2007. Re–Os isotope dating of molybdenites in the Huangshaping Pb–Zn–W–Mo polymetallic deposit, Hunan Province, South China and its geological significance. Sci. China, Ser. D 50, 519–526.
Yu, H.X., Liu, J.Y., 1997. The characteristic and petrogenesis of the granitic subvolcanic complex in the Shuikoushan orefield. Geotecton. Metallog. 21, 32–40 (in Chinese with English abstract).
Yuan, S.D., 2013. Molybdenite Re–Os dating for the Yulong skarn Mo deposit in Tongshanling orefield, southern Hunan. Geol. Rev. 59, 393–394 ((Supp), (in Chinese)).
Yuan, S.D., Wang, X.D., 2013. Zircon LA–(MC)–ICP-MS U–Pb dating and its implication for the Xianglinpu intrusion in Weijiawu district, southern Hunan. Acta Geol. Sin. 87, 62–64 ((Supp), (in Chinese)).
Yuan, S.D., Peng, J.T., Shen, N.P., Hu, R.Z., Dai, T.M., 2007. ^{40}Ar–^{39}Ar isotopic dating of the Xianghualing Sn–polymetallic orefield in southern Hunan, China and its geological implications. Acta Geol. Sin. 81, 278–286.
Yuan, S.D., Peng, J.T., Hu, R.Z., Li, H.M., Shen, N.P., Zhang, D.L., 2008. A precise U–Pb age on cassiterite from the Xianghualing tin–polymetallic deposit (Hunan, South China). Miner. Deposita 43, 375–382.
Yuan, S.D., Peng, J.T., Hao, S., Li, H.M., Geng, J.Z., Zhang, D.L., 2011. *In situ* LA–MC–ICP-MS and ID-TIMS U–Pb geochronology of cassiterite in the giant Furong tin deposit, Hunan Province, South China: new constraints on the timing of tin–polymetallic mineralization. Ore Geol. Rev. 43, 235–242.
Yuan, S.D., Zhang, D.L., Shuang, Y., Du, A.D., Qu, W.J., 2012a. Re–Os dating of molybdenite from the Xintianling giant tungsten–molybdenum deposit in southern Hunan Province, China and its geological implications. Acta Petrol. Sin. 28, 27–38 (in Chinese with English abstract).
Yuan, S.D., Liu, X.F., Wang, X.D., Wu, S.H., Yuan, Y.B., Li, X.K., Wang, T.Z., 2012b. Geological characteristics and ^{40}Ar–^{39} Ar geochronology of the Hongqiling tin deposit in southern Hunan Province. Acta Petrol. Sin. 28, 3787–3797 (in Chinese with English abstract).
Yuan, S.D., Mao, J.W., Cook, N.J., Wang, X.D., Liu, X.F., Yuan, Y.B., 2015. A Late Cretaceous tin metallogenic event in Nanling W–Sn metallogenic province: constraints from U–Pb, Ar–Ar geochronology at the Jiepailing Sn–Be–F deposit, Hunan, China. Ore Geol. Rev. 65, 283–393.
Zeng, N.S., Izawa, E., Motomura, Y., Lai, L.R., 2000. Silver minerals and paragenesis in the Kangjiawan Pb–Zn–Ag–Au deposit of the Shuikoushan mineral district, Hunan Province, China. Can. Mineral. 38, 11–12.
Zhang, Y.Z., 1957. The Shuikoushan Pb–Zn deposit in Hunan, China. Geol. Rev. 17, 310–323 (in Chinese).
Zhang, R.Q., Lu, J.J., Zhu, J.C., Yao, Y., Gao, J.F., Chen, W.F., Zhao, Z.J., 2010. Zircon U–Pb geochronology and Hf isotopic compositions of Hehuaping granite porphyry, southern Hunan Province, and its geological significance. Geol. J. China Univ. 16, 436–447 (in Chinese with English abstract).
Zheng, J.H., Guo, C.L., 2012. Geochronology, geochemistry and zircon Hf isotopes of the Wangxianling granitic intrusion in south Hunan Province and its geological significance. Acta Petrol. Sin. 28, 75–90 (in Chinese with English abstract).
Zhou, X.M., Sun, T., Shen, W.Z., Shu, L.S., Niu, Y.L., 2006. Petrogenesis of Mesozoic granitoids and volcanic rocks in South China: a response to tectonic evolution. Episodes 29, 26–33.
Zhu, X., 1999. Mine Situation in China (Volume II). Science Press, Beijing, pp. 1–665 (in Chinese).
Zhu, Y.L., Li, C.Y., Lin, Y.H., 1981. The Geology of Tungsten Deposit, Southern Jiangxi Province. Jiangxi People's Publishing House, Nanchang, pp. 1–440 (in Chinese).
Zhu, J.C., Zhang, H., Xie, C.F., Zhang, P.H., Yang, C., 2005. Zircon SHRIMP U–Pb geochronology, petrology and geochemistry of the Zhujianshui granite, Qitianling pluton, southern Hunan Province. Geol. J. China Univ. 11, 335–342 (in Chinese with English abstract).
Zuo, C.H., Lu, R., Zhao, Z.X., Xu, Z.W., Lu, J.J., Wang, R.C., Chen, J.Q., 2014. Characterization of element geochemistry, LA–ICP-MS zircon U–Pb age, and Hf isotope of granodiorite in the Shuikoushan deposit, Changning, Hunan province. Geol. Rev. 60, 811–823 (in Chinese with English abstract).